

短報

Automation of Routine Work in Athlete Support
Using Deep Learning MR Image Analysis Support Application
ディープラーニングによる MR 画像解析支援アプリケーションを用いた
アスリート支援におけるルーティンワークの自動化

Hiroki Ozaki¹⁾, Toshiharu Yokozawa¹⁾, Minoru Matsumoto¹⁾,
Wataru Ozaki²⁾, Shunji Miyauchi²⁾, Hideyuki Takahashi^{1),3)}
尾崎宏樹¹⁾, 横澤俊治¹⁾, 松本実¹⁾, 尾崎航²⁾, 宮内駿治²⁾, 高橋英幸^{1),3)}

Key words : fitness, trace, segmentation, cross-sectional area, AI

キーワード : フィットネス, トレース, セグメンテーション, 横断面積, 人工知能

I. Introduction

1. Current status and challenges of muscle morphometry using MRI.

The Japan Institute of Sports Sciences (from now on referred to as JISS) conducts muscle morphometry as a fitness assessment for top athletes to improve their international competitiveness²⁾. In principle, muscle morphometry in JISS involves calculating the cross-sectional area of the muscles and fat that make up the thighs and the lower trunk. In this measurement, the thighs and lower trunk are first imaged using a magnetic resonance imaging (MRI) machine. Then the boundaries of the muscle, fat, and bone components on the MR image are manually traced (segmented). The next step is to assign names to each of the divided components and calculate the cross-sectional area of each tissue. Although a series of tasks are carried out by well-trained support staffs (from now on referred as experts), there is a lot of manual work

involved, and it takes a lot of time from tracing to cross-sectional area calculation. In high performance sports, tailor-made assistance to athletes is required. In order to achieve this aim, it is important to create a system in which routine tasks including MR image tracing can be mechanized and more time can be spent on tasks that only support staffs can perform. In recent years, technologies related to artificial intelligence have improved dramatically⁴⁾. Among them, technologies using deep learning (from now on referred to as DL) that handle image processing are increasingly being used in the medical field⁷⁾. Therefore, it is expected that the above issues can be solved using DL analysis methods. However, no applications are available on the market to solve this problem. The JISS has more than 4,000 sets (as of March 2020) of segmentation data and MR images that have been traced to MR images of top athletes by experts, which can be used to prepare supervised data for the

¹⁾Japan Institute of Sports Sciences, ²⁾Hitachi Industry & Control Solutions, Ltd., ³⁾University of Tsukuba

¹⁾国立スポーツ科学センター, ²⁾日立産業制御ソリューションズ, ³⁾筑波大学

E-mail : hiroki.ozaki@jpnpsport.go.jp

受付日 : 2023 年 4 月 25 日

受理日 : 2023 年 12 月 18 日

development of applications using DL. In addition, as these data were from top athletes, it is possible to develop applications specifically for top athletes. Therefore, the purpose of this study is to develop a DL-based MR image analysis support application dedicated for top athletes to create an environment in which support staffs can focus on support that cannot be mechanized.

II. Development Overview

1. MR image segmentation models using DL.

In this study, we applied the DL methods in semantic segmentation to trace the MR images. Various models are available for semantic segmentation, including DeepLab v3 +¹⁾ and U-Net⁵⁾. Among other features, DeepLab v3 + is an extension of DeepLab v3 with a multilayer neural network architecture for semantic segmentation, with the added feature of being able to effectively extract object boundaries. The accuracy of the segmentation process near the boundaries of the objects is considered high and suitable for DL-based tracing. Therefore, this study examines the development of thighs and lower trunk semantic segmentation algorithm using DeepLab v3 + and its automatic rendering accuracy.

2. Dataset

In this study, 911 images of the thighs and 932 images of the lower trunk of several athletes taken at the JISS to date were used as supervised data. Consent for using images was obtained from all athletes at the time of their participation in the fitness assessment. This study was approved by the Ethics Committee of the Japan Institute of Sports Sciences (approval No. 2022-054). All MR images were acquired using a 3-Tesla superconducting MRI device (Magnetom Verio, Siemens, Germany) and a body coil. Transverse fast spin-echo image (matrix 256×256 , field of view 240 mm, thickness 10 mm) of the thigh was obtained at 50% position of the length between the trochanter

major and the tuberculum intercondylare. For the trunk, transverse gradient echo image (matrix 256×256 , field of view 380 mm, thickness 10 mm) was obtained at Jacoby's line, which connects on the superior border of the iliac fossas. To avoid motion artifacts attributable to breathing, MRI of the trunk was performed with the subjects holding their breath at the inspiratory position. Then, the obtained MR images was converted to 512×512 with interpolation processing. The dataset was used for DL training (Thighs: 806 images, lower trunk: 827 images) and evaluation (similarity assessment images were not used for training. Thighs: 105 images, lower trunk: 105 images). Regarding the dataset for evaluation, the images that were not suitable as evaluation images, including blurred images and artifact images, were thinned out, resulting in 58 images for the thighs and 79 images for the lower trunk. These MR images were manually labeled with labels traced and named by experts, with 11 labeling sites for the thighs (rectus femoris, vastus lateralis, vastus intermedius, vastus medialis, sartorius, lateral hamstring, medial hamstring, adductors, gracilis, fats, and bones) and 12 for the lower trunk (right and left rectus abdominis, Oblique, Psoas major, quadratus lumborum, erector spinae, as well as fats and bones)²⁾. The segmentation data for each site generated from the MR images and labels were paired to form a dataset. Fig. 1 shows examples of the images used in this study. These images were used to train and evaluate the model and study possible applications for automatic tracing using DL.

3. Interface

To solve this research problem, it needs to be implemented seamlessly in existing muscle morphometry analysis systems. Therefore, the interface developed in this study was designed to invoke the DL tracing process instead of conventional tracing operations. In addition, it was decided to retain the functionality that

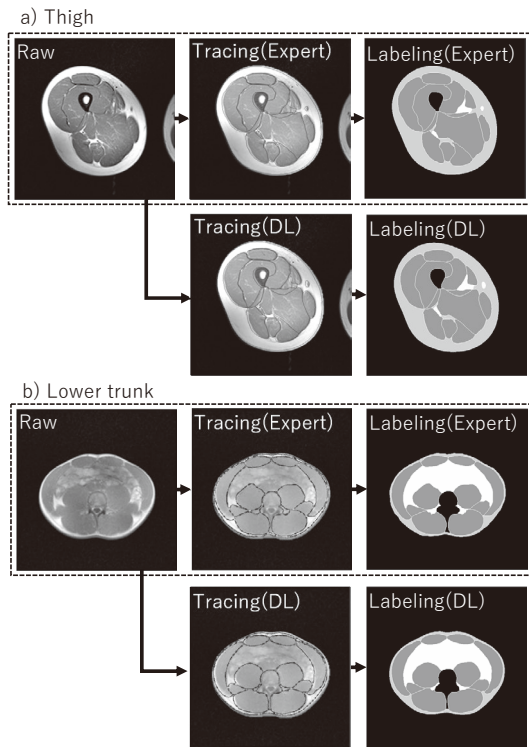


Fig. 1 Sample MR images used in this study.
a: MR image of the thighs and the corresponding tracing and labeling images.
b: MR image of the lower trunk and the corresponding tracing and labeling images.
Dashed lines indicate supervised data, and DL stands for deep learning. Gray: muscle; light gray: fats; white: blood vessels, nerves, internal organs, and others; black: bones.

allows manual tracing to be carried out in the same way as before without using the DL tracing process. Fig. 2 shows the timing of the tracing process using DL. The DL calculation model can be specified in the configuration file, and the input/output files are stored in folders to allow for future changes in the model and imaging area. The GPU used for the study was an NVIDIA Quadro RTX5000, an Intel Xeon W-2135 with a memory capacity of 64 GB.

4. Verification Methods

The DL tracing results for the MR images in the evaluation dataset were compared with those obtained by the experts. The similarity of the traced images

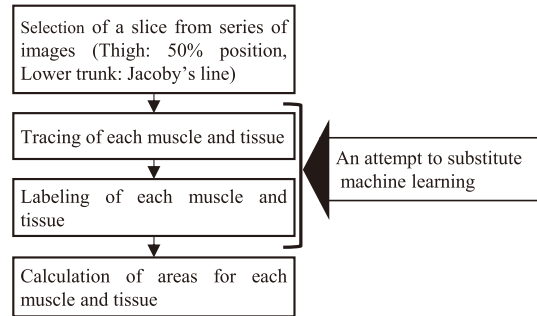


Fig. 2 Flow of calculating the area of each muscle and tissue from MRI images.

“Labeling” in Fig. 1) was verified using overlap-based metrics (Dice and Simpson coefficients)⁶⁾. The area of each muscle (group) and tissue was also validated by absolute error (the mean percentage of all samples of the absolute value of the error divided by the expert value), systematic error (the mean percentage of all samples of the DL value minus the expert value divided by the expert value), and the intraclass correlation coefficient (ICC). These metrics can be used to reveal areas of relatively low accuracy when segmenting the thighs and lower trunk by this model. This information would help support staff work more efficiently. The areas of the muscle groups in the lower trunk were summed on the left and right sides. The Adam³⁾ was used as the optimization algorithm for training the network, and the hyper-parameters, such as the learning rate, were tuned, resulting in a learning rate of 0.0005%, iteration of 400,000, batch size of 1, and time taken to train: approximately 300 h for the thighs. For the lower trunk, the learning rate was 0.0004%, iteration was 600,000, batch size was 1, and the time required for learning was approximately 300 h.

III. Verification results

The image similarity results are listed in Table 1. The Dice and Simpson coefficient s were above 97% for both the thighs and the lower trunk. The validation results for the area of each muscle and tissue in the

thighs and lower trunk are presented in Tables 2 and 3, respectively. For both muscles and tissues, absolute and systematic errors were less than 5%, with ICCs

Table 1. Overlap coefficients (%) for traced images between machine learning and expert person for the thighs and lower trunk.

| | | Mean | SD |
|-------------|---------|------|-----|
| Thigh | Dice | 97.6 | 1.8 |
| | Simpson | 98.5 | 3.1 |
| Lower torso | Dice | 97.2 | 1.9 |
| | Simpson | 98.4 | 3.0 |

greater than 0.9.

IV. Conclusion

After training the model using DeepLab v3+ with the dataset held by JISS, the Dice and Simpson coefficients were above 97% for both the thighs and lower trunk. In addition, both absolute and systematic errors were less than 5% for both muscles and tissues, and the ICC was greater than 0.9. Based on these results, it can be concluded that segmentation using the model developed in this study was highly accurate.

Table 2. Verification results for each muscle and tissue area of the thighs.

| | by DL (cm ²) | | by expert (cm ²) | | Absolute error (%) | | Systematic error (%) | | ICC |
|--------------------|-----------------------------|------|---------------------------------|------|-----------------------|-----|-------------------------|-----|-------|
| | Mean | SD | Mean | SD | Mean | SD | Mean | SD | |
| | Muscles | 85.5 | 17.4 | 85.2 | 17.3 | 0.4 | 0.3 | 0.3 | |
| Rectus femoris | 5.3 | 1.3 | 5.2 | 1.3 | 2.1 | 1.3 | 1.3 | 2.1 | 0.995 |
| Vastus lateralis | 15.3 | 3.7 | 15.3 | 3.7 | 1.1 | 0.7 | 0.3 | 1.3 | 0.999 |
| Vastus intermedius | 13.4 | 2.9 | 13.5 | 3.0 | 1.2 | 0.9 | -0.7 | 1.4 | 0.997 |
| Vastus medialis | 8.6 | 2.1 | 8.6 | 2.1 | 1.8 | 1.3 | -0.2 | 2.2 | 0.996 |
| Sartorius | 2.2 | 0.6 | 2.2 | 0.6 | 4.6 | 3.5 | 3.2 | 4.8 | 0.980 |
| Lateral hamstring | 8.1 | 1.7 | 8.0 | 1.7 | 1.7 | 1.4 | 0.8 | 2.1 | 0.995 |
| Medial hamstring | 10.4 | 2.4 | 10.3 | 2.5 | 2.4 | 1.7 | 1.4 | 2.6 | 0.993 |
| Adductors | 19.1 | 5.3 | 19.1 | 5.3 | 1.2 | 1.1 | 0.4 | 1.6 | 0.999 |
| Gracilis | 2.9 | 0.7 | 2.9 | 0.7 | 3.6 | 5.2 | 0.7 | 6.3 | 0.977 |
| Fats | 22.1 | 10.9 | 22.2 | 10.9 | 2.2 | 2.5 | -0.6 | 3.3 | 0.999 |
| Bones | 3.2 | 0.6 | 3.2 | 0.6 | 2.0 | 2.1 | 1.9 | 2.2 | 0.989 |
| All | 113.2 | 19.4 | 112.9 | 19.3 | 0.4 | 0.3 | 0.3 | 0.4 | 1.000 |

Table 3. Verification results for each muscle and tissue area of the lower trunk. The left and right values for the muscles were summed.

| | by DL (cm ²) | | by expert (cm ²) | | Absolute error (%) | | Systematic error (%) | | ICC |
|--------------------|-----------------------------|------|---------------------------------|------|-----------------------|-----|-------------------------|------|-------|
| | Mean | SD | Mean | SD | Mean | SD | Mean | SD | |
| | Muscles | 36.9 | 7.5 | 37.0 | 7.5 | 1.4 | 1.1 | -0.4 | |
| Rectus abdominis | 3.3 | 0.8 | 3.3 | 0.8 | 3.7 | 2.7 | -0.2 | 4.6 | 0.984 |
| Oblique | 11.6 | 2.8 | 11.8 | 2.9 | 2.6 | 2.0 | -1.9 | 2.7 | 0.990 |
| Psoas major | 7.3 | 2.1 | 7.2 | 2.0 | 3.2 | 2.4 | 1.4 | 3.7 | 0.992 |
| Quadratus lumborum | 3.2 | 0.8 | 3.2 | 0.7 | 4.7 | 4.4 | -0.8 | 6.4 | 0.972 |
| Erector spinae | 11.6 | 2.3 | 11.6 | 2.3 | 2.0 | 1.4 | 0.2 | 2.5 | 0.994 |
| Fats | 17.1 | 10.1 | 16.8 | 10.3 | 3.8 | 3.4 | 2.9 | 4.2 | 0.998 |
| Bones | 5.4 | 0.7 | 5.4 | 0.7 | 4.1 | 3.4 | 1.3 | 5.2 | 0.921 |
| All | 87.7 | 18.5 | 88.1 | 18.6 | 0.4 | 0.4 | -0.4 | 0.4 | 1.000 |

However, in the measurement of muscle morphology in top athletes, small errors may affect their training plan. Therefore, it is desirable to perform muscle morphometry measurements using this model for feedback after final confirmation by experts. Nevertheless, it was found that experts' work time could be reduced by approximately one-third in subsequent operations. This indicates that the application developed in this study allowed us to create an environment in which more human resources could be invested in support. However, there is concern that the use of this application by untrained support staffs in muscle morphometry may inhibit the transmission of tracing techniques. As a countermeasure, a system that allows those untrained support staffs to learn correct tracing by having the system judge the accuracy of the manual tracing results can be considered. Therefore, the operation of this system should be considered in the future.

References

- 1) Chen LC, Zhu Y, Papandreou G, Schroff F, Adam H. Encoder-decoder with atrous separable convolution for semantic image segmentation. *Eur Conf Comput Vis*, 801–818, 2018.
- 2) JAPAN SPORT COUNCIL. FITNESS CHECK HANDBOOK: assessments of physical fitness in athletes. TAISHUKAN, 2021.
- 3) Kingma DP, Ba J. Adam: A Method for Stochastic Optimization, arXiv preprint. <https://arxiv.org/abs/1412.6980>, 2014
- 4) Minaee S, Boykov Y, Porikli F, Plaza A, Kehtarnavaz N, Terzopoulos D. Image segmentation using deep learning: a survey. *IEEE Trans Pattern Anal Mach Intell*, 44 (7) : 3523–3542, 2022.
- 5) Ronneberger O, Fischer P, Brox T. U-net: Convolutional networks for biomedical image segmentation. *Med Image Comput Comput Assist Interv*, 234–241, 2015.
- 6) Taha AA, Hanbury A. Metrics for evaluating 3D medical image segmentation: analysis, selection, and tool. *BMC Med Imaging*, 15 (1) : 1–28, 2015.
- 7) Van Eetvelde H, Mendonça LD, Ley C, Seil R, Tischer T. Machine learning methods in sport injury prediction and prevention: a systematic review. *J Exp Orthop*, 8 (27), 2021.